Watching the Polymorphic Transition from a Field-Induced to a Stable Crystal by Dielectric Techniques

D. M. Duarte,[1,2] R. Richert[3] and K. Adrjanowicz [1,2]

[1] Institute of Physics, University of Silesia, 75 Pulku Piechoty 1, 41-500 Chorzow, Poland

[2] Silesian Center for Education and Interdisciplinary Research (SMCEBI), 75 Pulku Piechoty 1a, 41-500 Chorzow, Poland

[3] School of Molecular Sciences, Arizona State University, Tempe, Arizona 85287, USA

ABSTRACT

We prepared a metastable polymorph of vinyl ethylene carbonate by inducing crystallization of the supercooled liquid via an electric field of about 80 kV cm^{-1}. Electric fields with sufficiently low frequencies are required to observe polymorphism for this material. Depending on the temperature protocol prior to crystallization, the field-induced crystal structure can be obtained either with high polymorphic purity or mixed with seed crystals of the ordinary stable polymorph. At the crystallization temperature of T_c = 198 K, the pure field-induced polymorph shows no sign of a polymorphic transition, while at the same temperature, this crystal structure converts to the stable state in a matter of several hours if seeded by the stable polymorph. Interestingly, we find that the permittivity changes linearly with the volume fraction of the field-induced polymorph during the conversion, so that the polymorph transition can be followed in real-time by dielectric techniques.

Introduction

Polymorphs are distinct crystal structures that can be formed by the same chemical compound.[1,2] Numerous examples for polymorphism exist for organic molecular materials.[3,4,5] For instance, a compound known as ROY for its red, orange, and yellow crystals has seven polymorphs whose structures have been determined,[6] while computational approaches to the structures of this organic molecule suggest the existence of many more.[7] Polymorphic transitions are conversions from one metastable polymorph to a more stable one,[8] while retaining the chemical identity of the material. In the case of enantiotropic polymorphism, temperature affects which structure is the more stable one,[9] i.e., the polymorph with lower free energy. One complication has been recognized already a long time ago by Ostwald,[10,11] namely that a structural transition will not necessarily proceed to the lowest free energy state in a single step, but is likely to undergo a polymorphic transition that is associated with a smaller change in free energy.

Understanding the existence of polymorphs and the transitions among them is of great importance to materials science and relevant to societal issues in the case of pharmaceuticals. For example, the HIV protease inhibitor ritonavir was found to be subject to a polymorphic transition leading to a structure with highly compromised solubility and thus bioavailability.[12,13] Many other pharmaceuticals, as well as their precursors, are known to display polymorphism.[1,5,6,14,15] Although the molecular chemistry is the same, polymorphs of lower thermodynamic stability are usually associated with higher solubility and rate of dissolution, thus favoring bioavailability, but the shelf life of that structure might be limited.

The feature that creates different polymorphs in the first place is the variety of thermodynamic paths that impact nucleation and growth kinetics. Commonly, these are the temperature and/or pressure histories that the sample has undergone before settling at ambient conditions, for instance. It may be speculated that every compound is associated with polymorphism, but for many systems the thermodynamic path required to create a novel polymorph has not yet been found.[1] A less common route to forming new polymorphs is by applying an electric field of sufficient magnitude.[16,17,18,19,20,21]

In the case of vinyl ethylene carbonate (VEC), it has been demonstrated that a field gives rise to a new polymorph that melts about 20 K below the ordinary one and that has not been formed in the absence of a field.[22] Unfortunately, the crystal structures of both polymorphs are not know, because

both melt at temperatures far below ambient conditions. In order to discriminate these two structures unambiguously, we label the polymorphs as follows: The polymorph that is formed only in the presence of an electric field is named 'field-induced metastable' or 'metastable' (with melting temperature $T_{m,m} = 208.5$ K), and the ordinary one is referred to as 'stable' polymorph (with melting temperature $T_{m,s} = 227$ K). It is already established that a moderately high electric field accelerates the crystallization of VEC, leading to a field-induced metastable polymorph,[22] but only if the frequency of that field does not exceed a certain threshold.[23] Because the nucleation rate curves, $J(T)$, for the field-induced metastable and stable crystals have significantly different maxima positions on the temperature scale, the metastable or stable polymorph can be prepared in a targeted fashion.

This study focuses on the stability of the field-induced metastable polymorph, its potential polymorphic transition to the stable state, and the possibility of monitoring such a transition in real-time by dielectric techniques. At a temperature of T_c = 198 K, the supercooled liquid crystallizes within less than 2 hours into the metastable structure when subject to a field of $E \approx 80$ kV cm^{-1}. At the same temperature, we observe that this field-induced metastable polymorph transforms into the stable polymorph within a time frame of 15 hours if seeded by the ordinary crystal. By contrast, no such transformation is observed in the absence of seed crystals. Interestingly, the dielectric constant changes along with the progress of the polymorphic transition, so that the composition of the polymorph mixture can be monitored in real-time as the system changes the volume fraction of the more stable structure from practically zero to 100%.

Experiment

The compound 4-vinyl-1,3-dioxolan-2-one or vinyl ethylene carbonate (VEC, purity 99%) was obtained from Sigma-Aldrich and used as received. VEC is a vinyl derivative of propylene carbonate (PC) and has been referred to as 'vinyl-PC'. The liquid is loaded into a high-field capacitor cell described in detail in a previous publication (Fig. S1, supplementary information).[22] The polished parallel disks are made of stainless steel and are separated by a Teflon ring of $d = 25$ µm nominal thickness, leaving an active inner electrode surface area of $r = 7$ mm radius. The resulting geometric capacitance is $C_{geo} = \varepsilon_0 \pi r^2/d = 54.5$ pF. By comparing the observed permittivity with reference data, the actual electrode separation was determined to be closer to 20

μm. Temperature regulation of the sample cell was achieved by a Novocontrol Quatro temperature control system.

For dielectric measurements using large ac electric fields, a Trek PZD-700 high-voltage unit amplifies the output voltage of a Solartron SI-1260 gain–phase analyzer by a factor of 200. The current was measured via the voltage drop across a calibrated RC-shunt connected to the analyzer with a buffer amplifier that tolerates high voltages, employed to protect the system from sample failure. A schematic outline of the system is provided in Fig. 1a of a previous publication.[24] This setup can generate dielectric permittivity data, $\varepsilon = \varepsilon' - i\varepsilon''$, within the frequency range from 30 mHz to 120 kHz for fields up to 240 kV cm^{-1}. All voltage and field amplitudes are reported as root-mean-square (RMS) values. All fields intended to affect crystallization were around $E \approx 80$ kV cm^{-1}, while amplitudes of the alternating fields used to measure dielectric permittivity only were kept below 16 kV cm^{-1}, which is a factor of 25 lower in terms of nonlinear ($\sim E^2$) effects. Fields much below 80 kV cm^{-1} that are used only to measure the permittivity (without affecting the crystallization) are designated as "$E \approx 0$ kV cm^{-1}", regardless of their actual value.

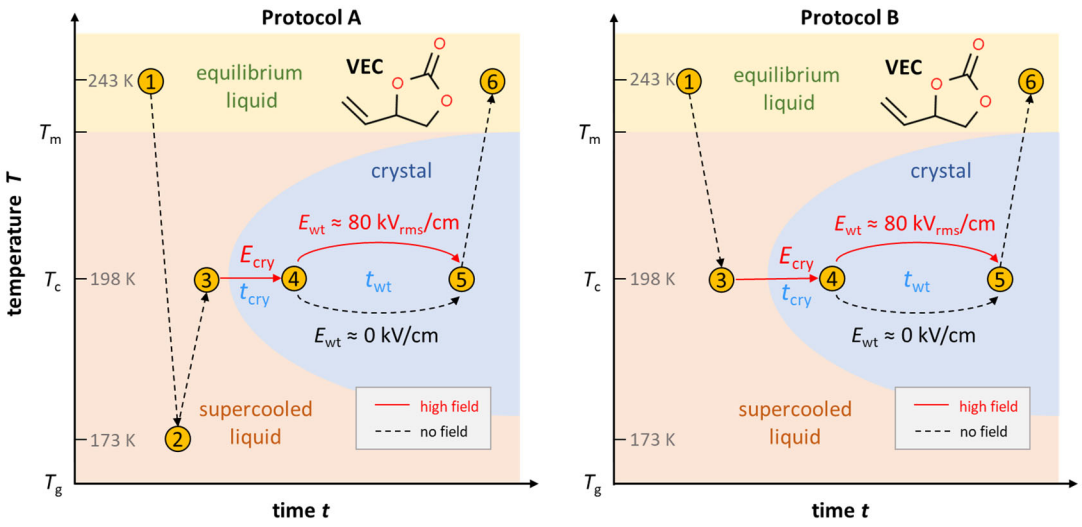

Figure 1. Schematic representation of the two different protocols used to prepare samples and record crystallization. Each case starts at the equilibrium liquid state (1) at $T = 243$ K $\approx T_m + 15$ K, and takes the sample to point (3), where the temperature is held at $T_c = 198$ K. Protocol 'A' inserts cooling to point (2) at $T = 173$ K $\approx T_g + 2$ K, whereas the temperature in protocol 'B' is never lower than $T_c = 198$ K. Crystallization occurs during the time interval t_{cry}, step 3 $\rightarrow$ 4, followed by a waiting time t_{wt}, step 4 $\rightarrow$ 5. Finally, the melting behavior is recorded during heating from $T_c = 198$ K back to $T = 243$ K, step 5 $\rightarrow$ 6. The yellow areas are for the equilibrium liquid (and include the molecular struture of VEC), beige is for the supercooled state, blueish grey is for the crystal formation domain, analogous to a time-temperature transformation (TTT) diagram.

Two distinct thermal protocols were used to generate VEC crystals at T_c = 198 K, both starting at the equilibrium liquid state at T = 243 K, which is approximately 15 K above the melting temperature of the stable (ordinary, low-field) polymorph. Schematic representations of these experimental protocols are provided in Figure 1. In the case of protocol 'A', the sample is cooled down to T = 173 K ≈ T_g + 2 K a rate of approx. 10 K min^{-1}, i.e., to just above the glass-transition region. The aim of this step is to induce nucleation of the stable polymorph, as nucleation rate maxima are often located close to T_g. Except for a few minutes needed for temperature stabilization, there is no waiting time at T = 173 K. Subsequently, the temperature is increased to T_c = 198 K at a rate of approx. 5 K min^{-1}. No field is applied prior to reaching T_c at point 3 in Figure 1. After reaching T_c, the sample is exposed to an ac-field of E ≈ 80 kV cm^{-1} at a frequency of ν = 5.62 Hz. Via dielectric spectroscopy, the progress of crystallization of VEC at T_c = 198 K is measured in the presence of the ac-field. Once the crystallization is completed, we have waited for some additional time (t_{wt} = 0, 3, 8.5, or 72 hours) with or without the ac-field remaining on. Afterward, the sample was heated at a rate of 1 K min^{-1} to T = 243 K while the changes in ε' at 10 kHz were monitored to detect melting events and determine the volume fraction of the crystalline materials.

In the case of protocol 'B', the sample is cooled down from T = 243 K at a rate of approx. 5 - 10 K min^{-1} directly to the crystallization temperature at T_c = 198 K without applying an electric field. This was done in order to avoid nucleation of the stable polymorph, as its nucleation rate is negligible for temperatures $T \geq$ 198 K. After reaching T_c, the sample is exposed to an ac-field of E ≈ 80 kV cm^{-1} of various frequencies or to a dc-field of the same amplitude. The progress of crystallization is monitored via the dielectric permittivity in the presence of the high electric field. Once the transformation to the crystalline state was completed, i.e., after t_{cry} has elapsed, an additional time t_{wt} may be added with the ac-field remaining on. Finally, the temperature is increased at a rate of 1 K min^{-1} to T = 243 K, while ε' at 10 kHz detects melting events and volume fractions of the polymorphs.

Results

The molecular liquid VEC belongs to the class of dipolar materials with negligible conductivity, such that electronic polarizability and orientational polarizability of the molecular dipoles are the main contributing features to the static dielectric constant, ε_s, which decreases mildly with

increasing temperature. At the fields used here, the effect of the field magnitude on the permittivity ε is negligible. The high frequency limit, ε_∞, of permittivity is governed by electronic polarizability and thus relatively independent of the structure, liquid or crystalline, and of temperature. Therefore, the progress of crystallization can be gauged by the real part of dielectric permittivity, ε', recognizing that only the volume fraction that is in the liquid state contributes to the orientational polarizability of permanent dipoles.[25] Thus, after subtracting ε_∞, the value of ε' relative to the static limit of the pure liquid, ε_s, is a good approximation to the volume fraction of the liquid in the sample:

$$V_{liq}/V_{total} = (\varepsilon' - \varepsilon_\infty)/(\varepsilon_s - \varepsilon_\infty)\ . \qquad (1)$$

Deviation from this relation due to dielectric mixing effects are sufficiently small to not interfere with the results of this study.[26,27] The frequency ν at which ε' is determined has to be sufficiently low such that the dipole orientation can follow the field with no time lag, which is he case for all frequencies used here. Various low frequencies (0.562 Hz ≤ ν ≤ 562 Hz) are employed to check the frequency dependence of the high field effect, ν = 10 kHz is selected for all melting curves because it allows for more robust results at higher data acquisition rates.

The results are shown separately for each protocol used, 'A' or 'B', the difference being that the stable polymorph is nucleated prior to crystallization in the 'A' case, whereas protocol 'B' is designed to avoid nucleation of the stable crystal form. For each protocol ('A' first, 'B' second') one graph depicts the crystallization behavior for different field conditions, and another shows the melting behavior of these crystalline sample, generally measured at practically zero field.

We begin with results obtained by following protocol 'A' of Figure 1, designed to nucleate the stable crystal via a temperature excursion to just above T_g before taking the sample to the crystallization temperature T_c = 198 K. For this protocol, the processes of crystallization at T_c = 198 K for different measurement conditions are shown in terms of ε' versus t in Figure 2, observed while the sample is subjected to a sinusoidal electric field of $E_{cry} \approx 80$ kV cm^{-1} at a frequency of ν = 5.62 Hz. As a point of reference, one curve for $E_{cry} \approx 0$ kV cm^{-1} is also included in Figure 2, where only a very low field is used to measure permittivity. For all curves in this figure, t = 0 has been defined as the onset of considerable crystallization, i.e. the extrapolated intersection between a more time invariant ε' plateau and the practically linear steep decline towards ε' = 3.6. After

reaching the target of T = 198 K at stage 3, the induction times are about 10^4 s for the field free case and typically less that 10^3 s for the application of 80 kV cm^{-1}, see the $t < 0$ range of Figure 2. Crystallization for the $E_{cry} \approx 0$ kV cm^{-1} case takes ε' rapidly to a level near 3.6, see inset of Figure 2, whereas all $E_{cry} \approx 80$ kV cm^{-1} curves terminate the rapid descent near a level of $\varepsilon' = 6.0$. Common to all $E_{cry} \approx 80$ kV cm^{-1} cases is the subsequent slow change from $\varepsilon' = 6.0$ to $\varepsilon' = 3.6$ in a near-linear fashion across about 14 hours. However, these curves differ in the wait time (t_{tw} = 0, 3, 8.5, or 72 h) during which the slow change has been recorded, which is relevant for the subsequent measurements, i.e., step 5 → 6 of protocol 'A'. For clarity, Figure 2 shows only results for which the field during the wait time has remained that applied during the crystallization phase, i.e., $E_{wt} = E_{cry}$. However, another such set of $E_{cry} \approx 80$ kV cm^{-1} curves has been recorded, but with $E_{wt} \approx 0$ kV cm^{-1}, cf. Figure 3.

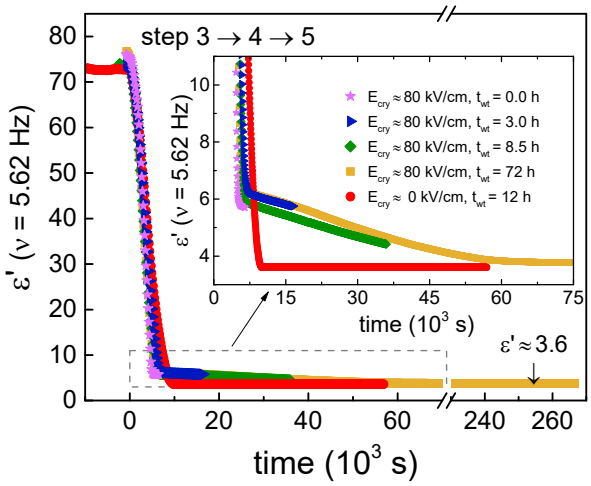

Figure 2. Time-dependent changes in dielectric permittivity ε' at a frequency ν = 5.62 Hz recorded for VEC in the presence of an ac-field E_{cry} as indicated in the legend. Prior to this measurement, the sample has followed steps 1 → 2 → 3 of protocol 'A' as illustrated in Figure 1. The drop of ε' signifies crystallization progress according to Equation (1). After complete crystallization, there is an additional waiting time t_{wt}, during which the ac field amplitude $E_{wt} = E_{cry}$ remains applied. The time dependence of ε' in the range 6 to 3.6 is shown on enlarged scales in the inset.

The results of Figure 3 are measured immediately following the end of the corresponding curves of Figure 2, all based upon a field that is within the linear response regime. The data represent $\varepsilon'(\nu_0$ = 10 kHz) recorded during a temperature scan from 198 to 243 K at a rate of about 1 K min^{-1}. Each curve starts at T_c = 198 K at a level that is equal to the end of the corresponding data set of Figure

2, indicative of practically complete crystallization. The main feature of Figure 3 is that an increase of the waiting time t_{wt} of step 4 → 5 leads to the amount of material melting already at $T_{m,m}$ = 208.5 K decreasing systematically. The comparison between open ($E_{wt} \approx 0$ kV cm^{-1}) and closed ($E_{wt} \approx 80$ kV cm^{-1}) symbols demonstrate that the magnitude of the field during the wait time has no effect on the melting outcome of Figure 3. Only two cases do not show any signs of melting the field-induced metastable (low-melting) polymorph at $T_{m,m}$ = 208.5 K, the case of crystallization in the absence of a high field ($E_{cry} \approx 0$ kV cm^{-1}), and the case of very long waiting periods (t_{wt} = 72 h).

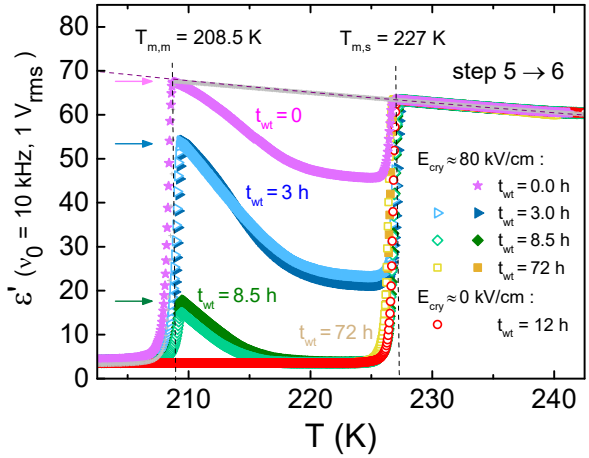

Figure 3. Temperature dependence of the dielectric permittivity ε' (at ν_0 = 10 kHz) measured on heating of the crystalline material obtained by following protocol 'A' and directly after the end of the traces of Fig. 2. With increasing waiting time t_{wt} at T_c = 198 K (step 4 → 5) the volume fraction of the field-induced metastable polymorph melting at $T_{m,m}$ = 208.5 K decreases, as it converts to stable form during t_{wt} which melts at $T_{m,s}$ = 227 K. Open symbols represent cases with $E_{wt} \approx 0$, solid symbols are for $E_{wt} \approx 80$ kV cm^{-1}, indicating the magnitude of E_{wt} has minimal effect on the volume fractions. The dashed curve indicates $\varepsilon_s(T)$, the arrows are explained in the text.

The remaining results are all derived from applying protocol 'B', where a deliberate nucleation of the stable polymorph has been avoided by cooling directly from $T > T_m$ to T_c, cf. Figure 1. In contrast to the protocol 'A' cases, protocol 'B' can lead to situations in which the sample resists crystallization for extended periods of time, because the stable polymorph had not been nucleated. This can be observed in Figure 4 for two curves whose ε' levels remain at ε_s for up to 22 h. Consistent with previous results, this can occur even for fields of E_{cry} = 80 kV cm^{-1}, provided that the frequency exceeds $\nu \approx 18$ Hz at T_c = 198 K,[23] see the ν = 562 and 56.2 Hz data in Figure 4.

Note that VEC also resists crystallization with protocol 'B' at zero field ($E_{cry} = 0$),[22,23] i.e., E_{cry} = 80 kV cm^{-1} at frequencies $\nu > 56.2$ Hz yields the same outcome as $E_{cry} = 0$. For all lower frequencies (including the dc cases, $\nu = 0$), crystallization leads to a rapid drop of permittivity values to around $\varepsilon' = 4.7$. Different wait times (with $E_{wt} = E_{cry} = 80$ kV cm^{-1}) have been applied to cases for which crystallization had occurred, i.e., for $\nu = 5.62$ Hz and $\nu = 0$, but the ε' level remains constant at 4.7 for up to 72 h.

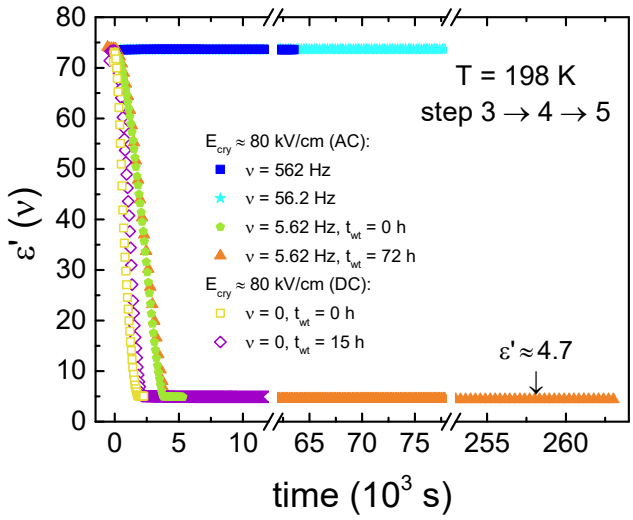

Figure 4. Time-dependent changes in dielectric permittivity ε' measured for various frequencies ν of the applied field of E_{cry} = 80 kV cm^{-1} for VEC at T_c = 198 K. Prior to this measurement, the sample has followed step 1 → 3 of protocol 'B' as illustrated in Figure 1. The drop of ε' signifies crystallization progress according to Equation (1). After complete crystallization, there is an additional waiting time t_{wt}, during which the field amplitude $E_{wt} = E_{cry}$ remains applied. The type of field (ac or dc), frequency ν, and waiting time t_{wt} are given in the legend. Crystallization of VEC at T_c = 198 K occurs only for sufficiently low frequencies.

Analogous to Figure 3, melting curves have been recorded for samples crystallized using protocol 'B', again by ramping temperature from T_c = 198 K to T = 243 K at about 1 K min^{-1}, directly after the end of the measurements shown in Figure 4. These results are compiled in Figure 5, which reveals that only one melting event is observed at $T_{m,m}$ = 208.5 K, regardless of high field frequency ($\nu \approx 5.62$ Hz versus $\nu \approx 0$) and wait time ($t_{wt} = 0$ versus $t_{wt} >> 0$). Furthermore, the inset of Figure 5 shows that whether the field is E_{wt} = 80 kV cm^{-1} or zero during the waiting time of t_{wt} = 72 h has no effect on melting for a sample crystallized at E_{cry} = 80 kV cm^{-1} with frequency ν = 0.562 Hz.

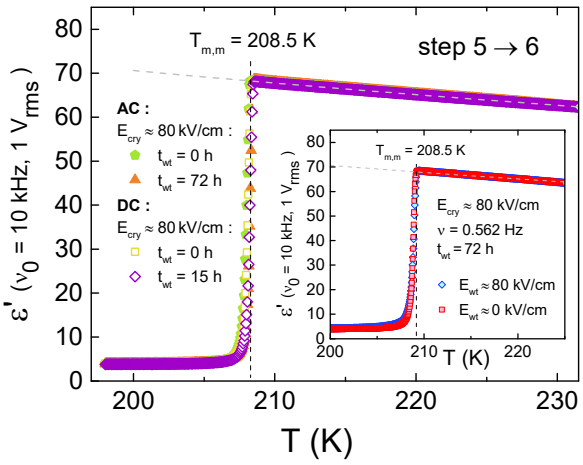

Figure 5. Temperature dependence of the dielectric permittivity ε' (at ν_0 = 10 kHz) measured on heating of the crystalline material obtained by following protocol 'B' and directly after the end of the traces of Figure 4. Melting occurs only at $T_{m,m}$ = 208.5 K, indicating 100% volume fraction of the field-induced metastable polymorph, regardless of waiting time t_{wt} and type of the high field, ac versus dc. The inset demonstrates that the magnitude of E_{wt}, 80 or 0 kV cm^{-1}, does not alter the stability of the field-induced metastable polymorph. The dashed curve indicates $\varepsilon_s(T)$.

Discussion

To our knowledge, polymorphic transitions from a field-induced metastable polymorph to the stable crystal structure that forms under ordinary conditions have not been studied to date. In this case of VEC, no polymorphism had been reported prior to applying an electric field, which led to a crystal structure that melts at $T_{m,m}$ = 208.5 K, located about 20 K below the regular melting point at $T_{m,s}$ = 227 K.[22] Based on that observation, one might speculate that electric fields may widen the range of materials exhibiting polymorphism, particularly with polar substances. Electric fields can modify the free energies relevant for nucleation and growth rates,[28,29,30,31] but only for polar particles is the interaction with the field sufficiently strong to impact crystallization.

The questions addressed in the following are concerned with how to stabilize the metastable polymorph, what are the time scales of polymorphic transformations, and can dielectric techniques monitor these transitions in real time. Before focusing on the polymorph transition and stability, a discussion of the field-effect on crystallization outcome and the resulting polymorph selectivity appears in order. Although the field effects such as accelerated crystallization and formation of a

metastable polymorph have been established earlier,[22,23] we confirm agreement with earlier observations for the present samples in the following sub-section.

Field effect. In order to clarify the impact of an electric field on the crystallization of VEC, we focus on the curves measured at low fields, $E_{cry} \approx 0$ kV cm^{-1}, and those obtained for $E_{cry} \approx 80$ kV cm^{-1} at zero wait time, $t_{wt} = 0$. According to Figure 2, both low and high field cases crystallize at about the same rate after the induction time ($t < 0$) has elapsed. The dominant field effect is revealed in Figure 3, where practically the entire volume fraction melts at $T_{m,s} = 227$ K for the $E_{cry} \approx 0$ case, whereas practically complete melting occurs at $T_{m,m} = 208.5$ K for the $E_{cry} \approx 80$ kV cm^{-1} and $t_{wt} = 0$ experiment. That these situations correspond to relatively high polymorphic purity in the crystalline state ($T < 205$ K in Figure 3) can be derived from the observation that the rise of ε' reaches ε_s (dashed curve in Figure 3) for each melting process, indicative of ≈100% liquid volume fraction after melting. For the field-induced metastable crystal melting at $T_{m,m} = 208.5$ K, subsequent crystallization for $T > T_{m,m}$ is the result of having nucleated the stable crystal with protocol 'A'. By comparison, the analogous set of curves obtained using protocol 'B' ($E_{cry} \approx 80$ kV cm^{-1} and $t_{wt} = 0$ in Figure 4 and Figure 5) show no such crystallization process above $T_{m,m} = 208.5$ K. That protocol 'B' suppresses nucleation of the stable crystal very effectively is confirmed by the $E_{cry} \approx 0$ case in Figure 4, where the liquid resists crystallization for 22 h.

As a result of the measurements discussed above, two distinct crystalline states of VEC with considerable polymorphic purity can be prepared: (1) the stable crystal using protocol 'A' without high electric fields, and (2) the field-induced metastable crystal using protocol 'B' while subjecting the sample to a high electric field of sufficiently low frequency. In the former case, no indication of a melting event at $T_{m,m} = 208.5$ K is observed, while the latter case does not show any formation of the stable crystal when heating above $T_{m,m}$.

These results are consistent with the picture of an electric field inducing a high nucleation rate of the metastable polymorph at $T_c = 198$ K, a temperature at which the nucleation rate of the stable polymorph is negligible. Therefore, the high electric field appears to open a new parallel crystallization route, without affecting nucleation and crystal growth rates of the stable crystal.

Polymorph transition. A subtle feature of the curves in Figure 2 is the variety of levels to which the ε' values fall in the course of crystallization if judged on the permittivity scale of the main

figure, $0 \leq \varepsilon' \leq 85$. The inset of Figure 2 emphasizes these features and clearly shows that the level reached during the first ≈ 2 h correlates strongly with the field E_{cry}: $\varepsilon' = 6.0$ for $E_{cry} \approx 80$ kV cm^{-1} and $\varepsilon' = 3.6$ for $E_{cry} \approx 0$. Therefore, according to Figure 2, the presence or absence of a considerable electric field during crystallization impacts the crystallization outcome in a qualitative fashion, with the zero field case crystallizing only the stable polymorph (red filled circles in Figure 2). For this protocol, it has been established that the low-field case gives rise to the stable polymorph, while the high field cases yield the new field-induced metastable polymorph. The interesting feature is that the permittivity transitions from $\varepsilon' = 6.0$ to $\varepsilon' = 3.6$ across a time window of about 14 h.

Now, one could speculate that these values $\varepsilon' = 6.0$ and $\varepsilon' = 3.6$ are the permittivities of the two distinct crystal structures, the field-induced metastable and the stable polymorph, respectively. However, in the absence of orientational degrees of freedom, these permittivities should be governed by molecular electronic polarizability and density and thus be much more similar for the two polymorphs. Therefore, it is too early to conclude that the change in ε' from 6.0 to 3.6 can be translated into a time-dependent volume partitioning of the two polymorphs. However, an independent approach to linking ε' to the volume fractions is via the levels observed after different waiting times, i.e., at the end of the traces in Figure 2. In the order of $t_{wt} = 0$, 3, 8.5, and 72 h, the ε' values reached at the end of the $E_{cry} \approx 80$ kV cm^{-1} curves in Figure 2 are 6, 5.5, 4.2, and 3.6, corresponding to x =100, 79, 26 and 0 % height if normalized to the 6.0 and 3.6 limits. These percentages are indicated as arrows in Figure 3, with their positions on the permittivity scale calculated as $\varepsilon = \epsilon_\infty + x(\epsilon_s - \epsilon_\infty)$. These levels provide a very good match with the volume fraction of the field-induced metastable polymorph as derived from the peak height of the melting process at $T = T_{m,m}$ relative to the limits ε_∞ and ε_s, cf. Equation (1). Therefore, it is justified to interpret the change of $\varepsilon'(t)$ from 6.0 to 3.6 (inset of Figure 2) as linearly related to the volume fraction of the field-induced metastable polymorph.

With the above reasoning, the statement of the waiting time dependence of Figure 2 is that the volume fraction $x_m = V_{\text{polymorph 'm'}}/V_{total}$ of the field-induced metastable polymorph decreases approximately linearly with time. The dependence can be approximated by $x_m = 1 - t/14h$ and is reproduced for the runs differing in t_{wt}, where $t = 0$ is defined by the kink near $\varepsilon' = 6$ in Figure

2. Such a linear time dependence of volume fraction is compatible with a growth-front like transformation process with time-invariant front velocities.[32]

Comparing the open ($E_{wt} \approx 0$) and solid ($E_{wt} \approx 80$ kV cm^{-1}) symbols in Figure 3, it can be observed that the presence of an electric field during the wait time has no impact on the polymorph transformation dynamics. It may seem reasonable to assume that the field would stabilize the field-induced metastable over the stable polymorph, but the orientational degree of freedom necessary for the field to lower the free energy is absent in the solid-state. Therefore, in contrast to the field being able to reduce the free energy of polar crystal nuclei suspended in the liquid,[23] the lack of crystallite orientation in a crystalline solid prevents such a field effect.

The feature responsible for the crystal type dependence of the dielectric constant, $\varepsilon' = 6.0$ versus $\varepsilon' = 3.6$, remains to be clarified. The level of $\varepsilon' = 6.0$ is hard to justify on the basis of reasonable values for electronic polarizability and density. A more likely cause for such high ε' numbers for a crystalline state is a residual amount of liquid or amorphous material between crystallites, the volume fraction of which may depend on the polymorph and crystallite sizes.

Polymorph stability. The previous section has demonstrated that the field-induced metastable polymorph can transform to the stable polymorph, cf. Figure 2 and Figure 3. It is important to realize that these transformation curves were obtained employing protocol 'A', cf. Figure 1, where a deliberate nucleation of the stable polymorph preceded the crystallization process under a field. This initial cooling to near T_g has a considerable effect on the stability of the field-induced metastable polymorph. That nuclei of the stable polymorph are present in the system subject to protocol 'A' even after field-induced crystallization and melting of the metastable polymorph is clearly seen by the crystallization that sets in for $T > T_{m,m}$ in Figure 3, even though their volume fraction is too small to show in the ε' data. A similar effect is absent in the case of protocol 'B', as no indication of crystallization for $T > T_{m,m}$ is found in Figure 5. Therefore, the system is practically free of nuclei of the stable polymorph when the sample is prepared using protocol 'B'.

Crystallization curves based on protocol 'B' are depicted in Figure 4, where crystallization sets in only when an electric field of sufficiently high amplitude and low frequency is applied. The ε' values rapidly drop to 4.6, and remain at that level for at least 72 h, with no indication of a polymorph transformation as outlined in the previous section. This reveals the much-increased stability of the field-induced metastable polymorph if prepared in the absence of nuclei of the

stable polymorph. The conclusion is that the polymorph transition requires seed crystals of the more stable crystal structure, analogous to the case of ritonavir,[12] where specks of the more stable crystal were found responsible for inducing the polymorphic transition to a form that resulted in the market withdrawal of the drug.

Summary and Conclusions

In the absence of an electric field, vinyl ethylene carbonate (VEC) has thus far shown only one crystal structure (the stable one) that melts at $T_{m,s}$ = 227 K, with no indication of polymorphism. At fields in excess of about E = 40 kV cm^{-1},[22] and with sufficiently low frequency,[23] VEC crystallizes into a field-induced metastable polymorph that melts at $T_{m,m}$ = 208.5 K. This study focuses on the polymorphic transition from the field-induced metastable to the stable crystal structure. It turns out that the field-induced metastable polymorph can be nucleated and grown efficiently at a temperature, T_c = 198 K, at which the nucleation rate of the stable polymorph is negligible (protocol 'B'). As a result, this field-induced metastable crystal structure can be obtained with high polymorphic purity, and in this case the metastable crystal displays no indication of a transformation for 72 h at T_c = 198 K, where crystal growth of the stable polymorph can be completed within about 2 hours.

The situation regarding the stability of the field-induced metastable polymorph changes when protocol 'A' is employed, where approaching T_g nucleates the stable polymorph, which remains as undetected volume fraction of seeds after an electric field turned practically the entire sample into the metastable polymorph. In this case, a polymorphic transition is observed, and the volume fraction of the stable structure increases linearly from ≈ 0 to ≈ 100 % within a time window of 14 h at T_c = 198 K. This result is independent of the electric field remaining on or switched off for the duration of this transition, indicating that the field-induced metastable polymorph cannot be stabilized via the field that promoted its nucleation. Interestingly, the dielectric permittivity changes linearly with the volume fractions during this transformation process, which allows for a direct observation of the polymorphic transition in real time.

It seems reasonable to assume that polymorphic transitions can be monitored by dielectric techniques also for other materials, i.e., for polymorphs that have not been obtained by the application of high electric fields. Metastable crystal structures of pharmaceuticals may be

advantageous with regards to bioavailability, but only if the shelf life is not cut short by a polymorphic transition. The present study underlines the importance of polymorphic purity for increasing the shelf-life of metastable crystal structures.

Acknowledgments

Part of this work was supported by the National Science Foundation under Grant No. DMR-1904601. Financial support from the National Science Centre within the framework of the SONATA BIS project (Grant No. 2017/26/E/ST3/00077) is greatly acknowledged.

References

(1) Bernstein, J. *Cryst. Growth Des.* **2011**, *11*, 632–650.

(2) Cruz-Cabeza, A. J.; Bernstein, J. *Chem. Rev.* **2014**, *114*, 2170–2191.

(3) Svärd, M.; Nordström, F. L.; Hoffmann, E.-M.; Aziz. B.; Rasmuson, Å. C. *Cryst. Eng. Comm.* **2013**, *15*, 5020–5031.

(4) Heinrich, M. A.; Pflaum, J.; Tripathi, A. K.; Frey, W.; Steigerwald, M. L.; Siegrist, T. *J. Phys. Chem. C* **2007**, *111*, 18878–18881.

(5) Nogueira, B. A.; Castiglioni, C.; Fausto, R. *Comm. Chem.* **2020**, *3*, 34.

(6) Yu, L. *Acc. Chem. Res.* **2010**, *43*, 1257–1266.

(7) Habgood, M.; Sugden, I. J.; Kazantsev, A. V.; Adjiman, C. S.; Pantelides. C. C. *J. Chem. Theory Comput.* **2015**, *11*, 1957–1969.

(8) Anwar, J.; Zahn, D. *Adv. Drug Deliv. Rev*. **2017**, *117*, 47–70.

(9) Vorländer, D. *Z. Phys. Chem.* **1923**, *105U*, 211–254.

(10) Ostwald, W. *Z. Phys. Chem.* **1897**, *22U*, 289–330.

(11) Schmelzer, J.; Möller, J.; Gutzow, I. *Z. Phys. Chem.* **1998**, *204*, 171–181.

(12) Bauer, J.; Spanton, S.; Henry, R.; Quick, J.; Dziki, W.; Porter, W.; Morris, J. *Pharm. Res.* **2001**, *18*, 859–866.

(13) Morissette, S. L.; Soukasene, S.; Levinson, D.; Cima, M. J.; Almarsson, Ö. *Proc. Natl. Acad. Sci.* **2003**, *100*, 2180–2184.

(14) Clout, A. E.; Buanz, A. B. M.; Gaisford, S.; Williams, G. R. *Chem. Eur. J.* **2018**, *24*, 13573–13581.

(15) Barbas, R.; Martí, F.; Prohens, R.; Puigjaner, C. *Cryst. Growth Des.* **2006**, *6*, 1463–1467.

(16) Evans, G. J. *Mat. Lett.* **1984**, *2*, 420–423.

(17) Taleb, M.; Didierjean, C.; Jelsch, C.; Mangeot, J. P.; Capelle, B.; Aubry, A. *J. Cryst. Growth* **1999**, *200*, 575–582.

(18) Hammadi, Z.; Veesler, S. *Prog. Biophys. Mol. Biol.* **2009**, *101*, 38–44.

(19) Nanev, C. N.; Penkova, A. *J. Cryst. Growth* **2001**, *232*, 285–293.

(20) Aber, J. E.; Arnold, S.; Garetz, B. A.; Meyerson, A. S. *Phys. Rev. Lett.* **2005**, *94*, 145503.

(21) Di Profio, G.; Reijonen, M. T.; Caliandro, R.; Guagliardi, A.; Curcio, E.; Drioli, E. *Phys. Chem. Chem. Phys.* **2013**, *15*, 9271–9280.

(22) Adrjanowicz, K.; Paluch, M.; Richert, R. *Phys. Chem. Chem. Phys.* **2018**, *20*, 925–931.

(23) Duarte, D. M.; Richert, R.; Adrjanowicz K. *J. Phys. Chem. Lett.* **2020**, *11*, 3975–3979.

(24) Pathak, U.; Richert, R. *Colloid Polym. Sci.* **2014**, *292*, 1905–1911.

(25) Böttcher, C. J. F. *Theory of Electric Polarization, Vol. 1*; Elsevier: Amsterdam, 1973.

(26) Jensen, M. H.; Alba-Simionesco, C.; Niss, K.; Hecksher, T. *J. Chem. Phys.* **2015**, *143*, 134501.

(27) Adrjanowicz, K.; Richert, R. Control of Crystallization Pathways by Electric Fields. In *Dielectrics and Crystallization*, Ezquerra, T. A.; Nogales, A., Eds.; Springer: Cham, 2020.

(28) Gutzow, I.; Schmelzer, J. W. P. *The Vitreous State: Thermodynamics, Structure, Rheology, and Crystallization*; Springer: Berlin, 2013.

(29) Kashchiev, D. *J. Cryst. Growth* **1972**, *13/14*, 128–130.

(30) Kashchiev, D. *Phil. Mag.* **1972**, *25*, 459–470.

(31) Isard, J. O. *Phil. Mag.* **1977**, *35*, 817–819.

(32) Swallen, S. F.; Traynor, K.; McMahon, R. J.; Ediger, M. D.; Mates, T. E. *Phys. Rev. Lett.* **2009**, *102*, 065503.